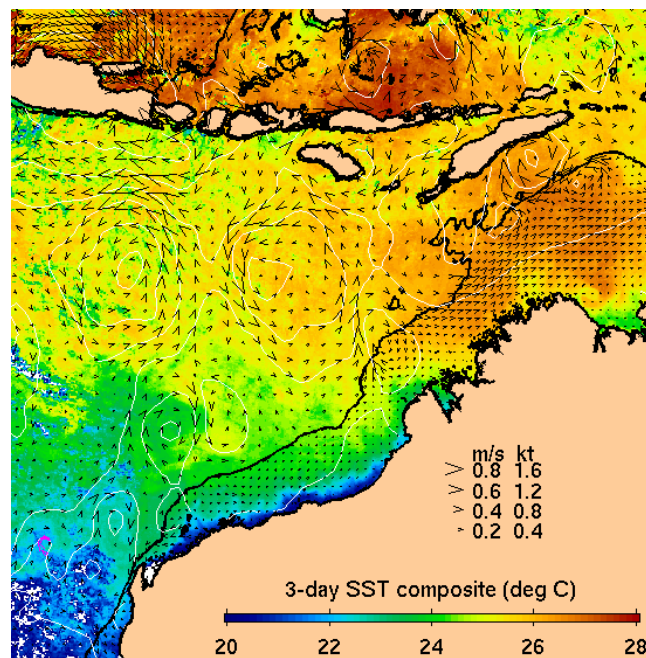


Nature of Intra-Seasonal Energy Propagation in the Indonesian Throughflow Region



Research internship report

March – July 2006



Emmanuel Vincent
Supervised by Dr Susan Wijffels



The present document is the report of an internship at CSIRO¹ Marine and Atmospheric Research in Hobart (Australia) performed by Emmanuel Vincent under the supervision of Dr Susan Wijffels. This internship spanned March to July 2006 and is part of the first year Master degree at “Terre-Atmosphère-Océan” department of the Ecole Normale Supérieure (Ulm, Paris).

Abstract

At tropical latitudes the Indonesian region allows water to exchange between the Pacific basin and the Indian Ocean. On average water leaves the west Pacific warm pool and travels to the Indian Ocean: this current is called the Indonesian Throughflow (ITF). Variability in the intra seasonal band is strong in the ITF region. This variability is known to temporarily reverse the Throughflow and likely affects ocean productivity in the region. It may be forced by both local and remote winds. We propose to combine new *in situ* mooring data and remotely sensed satellite sea level and winds data to characterise the intraseasonal events occurring during the first field phase of INSTANT, a new ITF mooring experiment. We hope to document the origin of these events, how their energy scatters through the region and affect the Indonesian Throughflow.

Résumé

Aux latitudes tropicales la région Indonésienne constitue le seul point de passage pour les échanges de masses d'eau entre le bassin Pacifique et l'Océan Indien. Le flot moyen dirigé depuis la piscine d'eau chaude du Pacifique Ouest vers l'Océan Indien est appelé “Courant Trans Indonésien (CTI)” (Indonesian Throughflow). La variabilité intra saisonnière du courant est importante dans cette région et est connue pour inverser temporairement le flot moyen ce qui a des répercussions sur la productivité des mers indonésiennes. Les causes probables de cette variabilité sont les forçages par les vents locaux ou distants.

Cette étude propose de combiner les nouvelles données issues des mouillages déployés lors de la première phase du programme INSTANT ainsi que des données de télédétection (vent de surface et altimétrie) afin d'étudier les événements inversant le CTI. Le but avoué de cette étude est de trouver l'origine des événements caractérisant la variabilité intra saisonnière et de comprendre comment leur énergie diffuse dans la région indonésienne Sud.

¹ Commonwealth Scientific and Industrial Research Organization

Table of content

Abstract	1
Résumé	1
Table of content.....	2
How to read this report.....	3
1. Geographic, Climatic and Scientific context	4
1.1. Characteristics of the Indonesian seas	4
1.2. What is the Indonesian Throughflow?.....	5
1.3. What climatic importance does the ISV have in the region?	5
Scientific context of this study and its purpose	5
2. Pre-processing the data.....	7
2.1. Spatial settings.....	7
2.2. Checking for errors due to the sensors	7
2.3. Project the velocity along the direction of the strait.....	8
2.4. Frequency filtering and bandpassing.....	8
2.5. Define a unique time base.....	12
Conclusion	12
3. The variability by mooring.....	13
3.1. Means, trends and variance	13
3.2. Temporal structure of the series	14
3.3. Frequency spectra: Power Spectral Density	15
3.4. Coherence spectra within each mooring.....	17
Conclusion	19
4. The variability in the region	20
4.1. Comparing the series between moorings	20
4.2. Coherence between moorings.....	21
Conclusion	21
5. Origin of the variability.....	23
5.1. Spatial correlation with the wind stress.....	23
5.2. The ‘May-2004 Event’	29
Conclusion	32
6. Conclusion, Perspectives for later researches	33
Acknowledgments:	34
References:	34
Annex.....	35

How to read this report

The two first parts are preliminary studies: a first part introduces the region and scientific context in which the study takes place and the second part presents the preparation of the data prior to analyses.

Part three and four describe the first approaches to characterise and understand the Intraseasonal Variability (ISV) of the variables within each strait and throughout the region. Eventually the fifth part researches the forcings responsible for the ISV observed in the region and tries to explain the mechanisms of the events constituting part of this variability.

In each section where necessary a first box indicates the **purpose** of the current part within the whole study and another box gives further information on the **methods** used and the mathematics of the operations performed on the data.

Throughout the study we comment on results regarding the variables measured in the straits, paragraphs commenting the temperature will begin with the **T** mark, paragraphs for velocity will begin with this one **ASv**.

1. Geographic, Climatic and Scientific context

1.1. Characteristics of the Indonesian seas

The area studied is located within the largest group of islands on Earth, these thousand of islands define many seas and numerous passages providing a route for the water to travel through the region (Indonesian seas contain Sulu, Savu, Celebes, Molucca, Java, Banda and Flores Seas, we can also attach the southern Arafura and Timor seas which mark the separation between Indonesia and Australia *see maps below*).

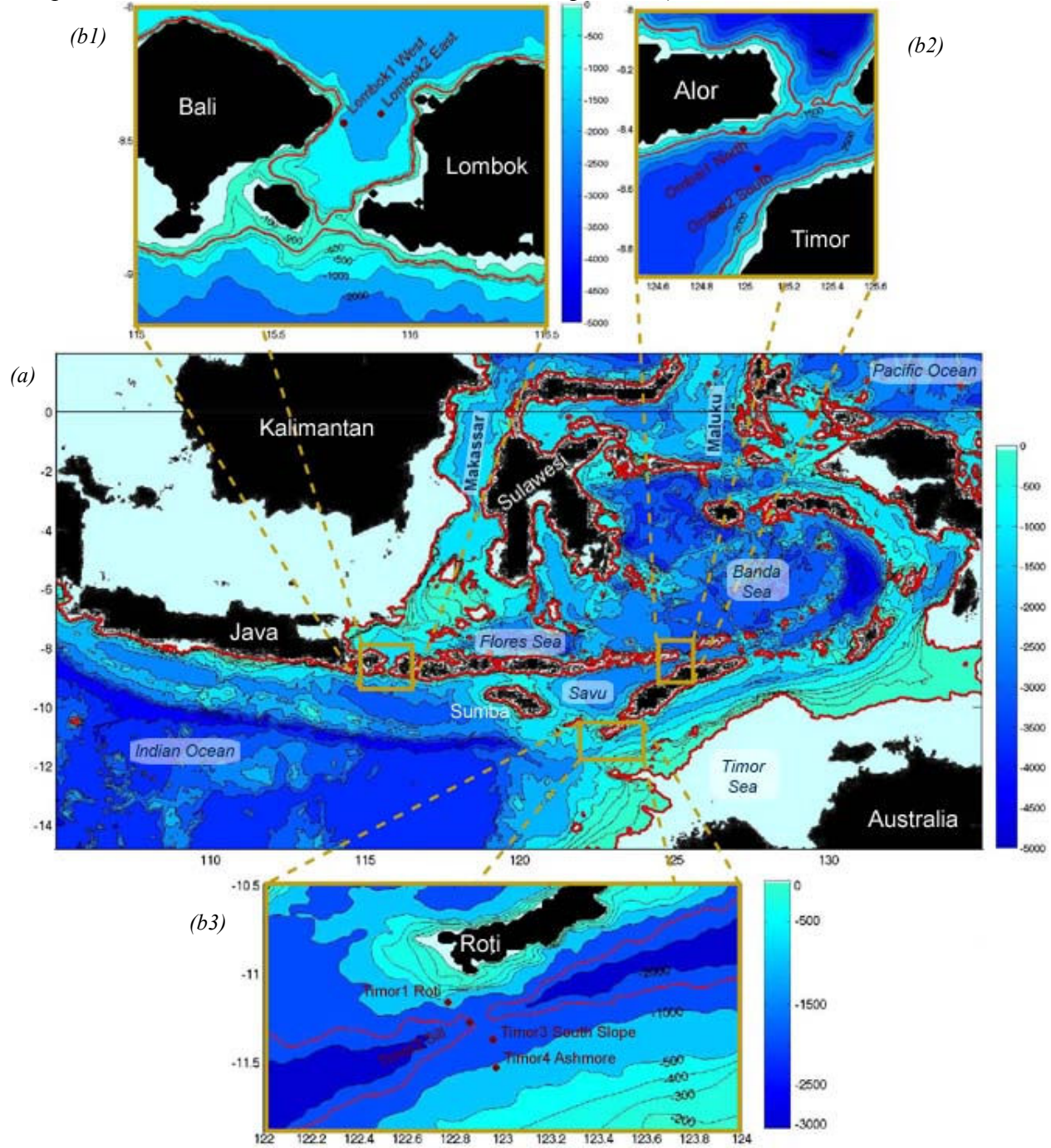


Fig 1.1 – Bathymetry of the region (a) showing red contour of the 100m depth; zoomed maps of the straits studied: Lombok (b1), Ombai (b2), Timor (b3) showing red contours respectively of the 280m, 1400m, 1550m depth. Data source: GEBCO bathymetry.

The 100m isobath shows the narrow passages where significant exchange can take place between the two basins. There are only few passages located at Makassar and Maluku Strait, for the inflow and at Lombok, Ombai, Timor Strait for exit flow. These straits are characterised by a 280m-deep sill in Lombok, a 1400m-deep sill north and a 800m-deep sill West (into Sawu Sea) in Ombai and a 1550m-deep sill in Timor (these depths have to be taken with care since the bathymetry in the region still has to be updated).

1.2. What is the Indonesian Throughflow?

The Indonesian Throughflow (ITF) is « the leakage of western tropical Pacific water into the south eastern tropical Indian Ocean through the Indonesian seas »^[2]. Because the “warm pool” is a place of heavy precipitation the ITF carries warm and relatively fresh water affecting both the basin budgets of the Indian and Pacific Oceans. From a broader point of view the ITF affects the Indo-Pacific warm pool by cooling the Pacific and warming the Indian Ocean.

Velocities in the channels may be affected by several factors among which the wind forcing over the Indian and Pacific Ocean. These remote winds generate long waves that propagate into the ITF region and affect variability at many time scales including the intraseasonal^[7].

1.3. What climatic importance does the ISV have in the region?

IntraSeasonal Variability (hereafter ISV) is the energy left when we subtract the annual (and longer), semi-annual, inertial and tidal (fluctuations with a period shorter than 10 days) frequencies. The Madden-Julian Oscillation is an example of the ISV in the atmosphere^[7].

One debated question is the roles ISV play in longer time scale variability like El Niño Southern Oscillation (ENSO). Kessler^[7] sums up these perceptions by the question: « Is ENSO a disturbance to a stable background state or a self-sustained mode on an unstable background? ». In the second scenario ENSO is seen as a quasi cyclic mode of oscillation of the Pacific climate system and ISV is a noise that exists on top of El Nino cycle but it is not fundamental to it. If we consider the first scenario, ENSO would be an initial value problem (each event is independent from the others) and ISV could be a potential initiating perturbation of an ENSO event. The variability of the ITF creates heat exchanges which could be related to the initiation of longer time scale variability by non-linear processes.

The South Equatorial Current in the Indian Basin is partly driven by the flow in Timor passage; thus the variability of the Indian Ocean circulation is related to some extent to the variability of the ITF. We could question the role of ISV in the Indian Ocean Dipole (equivalent of ENSO on the Indian Basin).

Scientific context of this study and its purpose

International Nusantara Stratification and Transport (INSTANT) program is an international array to directly measure the Indonesian ThroughFlow (ITF) and evaluate the variability and the importance of the exchanges between the two oceans. It involves scientists from Indonesia, Netherlands, France, United States and Australia. Its purpose is to understand the ISV of the flow in the straits between the Indonesian Seas and Indian Ocean. It aims to identify the forcings which determine ISV and to figure out how the energy associated with this/these forcing(s) propagate(s) into the region.

We use temperature and velocity measured at different depths throughout 18 months in the straits from the first phase of the INSTANT program which aims to collecting the data for 3

years. We also use remotely sensed wind speeds and sea level from ERSs to track the origin of the propagating phenomena affecting the ITF region.

2. Pre-processing the data

2.1. Spatial settings

Purpose

Associate the data with their location and depth

When we first have access to the data they are given by instrument, thus we need to create the data-set for each mooring and for each variable measured (temperature, eastward and northward velocity) and associate them with their serial number and percent good measures (see 2.2 checking for errors).

We need data at constant depths, but as the currents are very strong in the straits the moored instruments underwent large depth changes. Most sensors are equipped with pressure gauges that report the depth. Thus we have each measure associated with its true depth and we can interpolate in the vertical to find the temperature and velocity profile throughout the water column at each date. We assumed linear trend between measurements to interpolate this profile. A better way to find the variables on the vertical would be to use ocean vertical modes to interpolate taking into account the density profile. This depth grid is designed in each mooring with more points around the depth for which we have a good coverage of sensors.

Remark: The main variations of depth occur around 6 and 12 hours periods which correspond to the tides, but since we are interested in longer variability this is a good aspect (if well corrected) because it gives information at varying depths at a faster sampling rate than the changes we expect in the frequency band of interest.

2.2. Checking for errors due to the sensors

Purpose

To work only on data with a real physical significance

A first glance at the raw data plots of pressure shows us the oscillations associated with the tides (annex-1) but some sensors present on top of this feature a temporal trend. The first hypothesis if the trend affects the whole mooring is that the anchor is moving; indeed sometimes the anchor is set on steep floor. If the trend affects several sensors the reason is that they are moving because they slide along the axis or because the line is stretching. The previous cases don't need any correction since the values are estimated at the true depths (even if changing). If only one sensor behaves strangely, for instance introducing a trend in temperature not seen in surrounding instruments, then we assume that the sensor has drifted and we have to correct the values by removing the trend.

Velocity data from the Acoustic Doppler Current Profiler (ADCP) may contain several types of errors. The velocity is estimated from the frequency shift of an acoustic pulse reflected by particles moving with the water. Part of the pulse reflects off the surface toward the sensor which often is recorded with a low "percent good" warning. We chose to look only at the records showing a quality factor of 35 percent or more.

Velocity direction is evaluated from a compass present in the velocity sensors. Bad behaviour of the compass may happen modifying the eastward and northward components ratio. This error can be tracked by checking for unexpected behaviour of the velocity couple (u,v) with depth. The correction consists in suppressing the fake "rotation effect" in (u,v).

2.3. Project the velocity along the direction of the strait

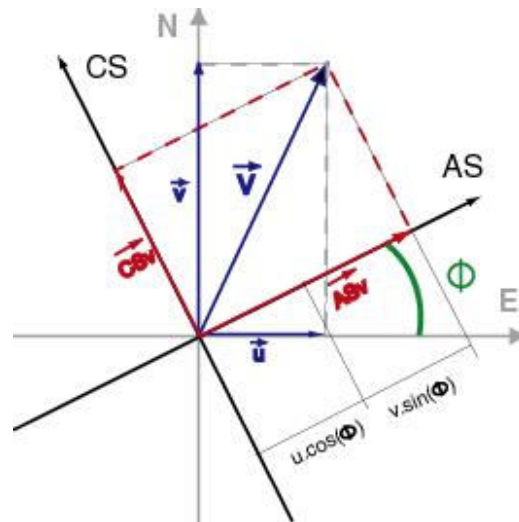
Purpose

Summarize the information, taking into account the maximum of variance

One operation to perform before going ahead on analysis is to project the (u,v) velocity from the East-West / North-South directions into Along-Strait / Cross-Strait coordinates (ASv,CSv). Given that the currents are mainly directed along the strait we ignore the cross-strait component. The method we used is to find the mean direction of the current in each 100m-depth layer and then average the direction of all these layers (shallow water are better sampled but we want to take into account all depths).

The projection on the along strait direction is performed as follow:

$$\begin{cases} ASv = u \cdot \cos(\phi) + v \cdot \sin(\phi) \\ CSv = -u \cdot \sin(\phi) + v \cdot \cos(\phi) \end{cases}$$



Remark that ASv is taken positive toward the East and North.

Fig 2.1 – Projection of velocity on the Along Strait direction

The percentage of variance of the total current explained by the Along Strait component is shown in Table 1. We remark that in Timor South moorings we can't really extract a major component while we can in other moorings.

Lombok1	Lombok2	Ombai1	Ombai2	Timor1	Timor2	Timor3	Timor4	Sunrise
90.5%	81.4%	91.9%	95.0%	87.7%	83.4%	53.3%	57.3%	87.7%

Table 1 – Percentage of total variance supported by the Along-Strait component

2.4. Frequency filtering and bandpassing

The standard deviation of our variables is dominated by the tides: for instance 68 percent of the variance of the temperature at 175m in Lombok West is to be attributed to tidal and inertial variability. Hence if we want to study longer period variations we need to filter the data.

Remark: We've mentionned that strong intraseasonal events may reverse the main flow in the straits, but we also have to keep in mind that tides reverse the flow with a 12 hours period on the whole depth.

There are two major ways of filtering (2.4.a and 2.4.b)

Method 2.4.a - Smoothing the time series with a running-mean filter ^[5]

The simplest method to suppress high frequencies consists in applying a running-mean filter which will smooth the time series, by choosing the appropriate length of the filter we can eliminate selected high frequencies. One problem with this technique is the loss of power generated: because we smooth the whole time series, we reduce the amplitude of all strong events even if they belong to a lower frequency.

Another similar technique is to apply a window function which will compute a weighted mean of the original time series suppressing chosen frequencies, one advantage is that we take into account a longer time span around the point we evaluate so we don't lose the trend when we evaluate the value at one date.

With these first approaches we process the signal without assuming that we know exactly the frequencies we want to suppress.

Method 2.4.b - Fitting the signal to a sinusoidal model

Another way to suppress specific frequencies when we know they are in our signal (tides, inertial frequency as a function of latitude, annual and semi-annual cycles) is to fit the time series to a sinusoidal function at the corresponding frequency by a least square method; then we subtract this fit from the original time series. The advantage of this method is that it is very specific and doesn't affect the data at others frequencies, we also don't lose energy in the signal.

$$x(t) \text{ being our time series and } A = \begin{bmatrix} \sin(2\pi \Delta t / T_A) \\ \cos(2\pi \Delta t / T_A) \\ \sin(2\pi \Delta t / T_{SA}) \\ \cos(2\pi \Delta t / T_{SA}) \end{bmatrix} \text{ we search } \alpha_j \text{ to minimise } (A \cdot \alpha_j - x)^2$$

α_j are the coefficients of the annual and semiannual cycles.

(see annex-2 time series before and after seasonal frequencies removed)

2.4.1. Removing high frequencies and annual cycle

Both temperature and velocity time series were treated similarly. The method we used was developed by Thompson (1981) ^[4]; it uses both approaches described in Method 2.4.a and 2.4.b: we fit the series to a sinusoidal signal at the tidal and inertial frequencies and we also apply a running mean to kill all the energy at period shorter than 1 day.

To check the efficiency of our filter we can first have a look at the series before and after the operation in the time domain (Fig 2.2).

Another way to check is to look in the frequency domain (annex-3). We verify that the fluctuations with a period greater than 2 days are suppressed and we don't lose power in other frequencies.

Wind stress and altimetry data analysed later were already averaged to daily (wind stress) or weekly (altimetry) sampling. We also suppress the annual and semi-annual variability in the time series using the method described in 2.4.b: Annual and semi-annual sinusoids were fitted and subtracted to remove the seasonal cycles (annex-2).

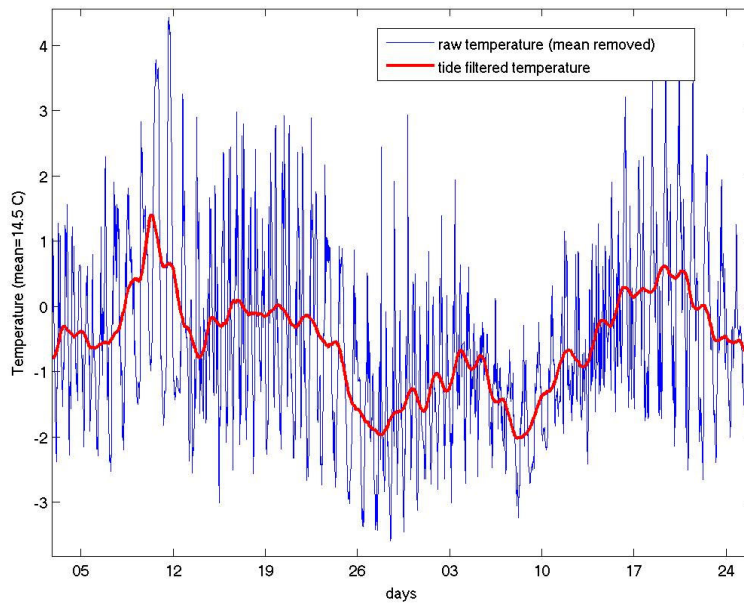


Fig 2.2 – Temperature before and after applying high frequency filter (Lombok W 175m)

2.4.2. Splitting the signal in frequency bands

Purpose

To give us the option to study the time series only within the bands of frequency corresponding to a given physical process

Following considerations of previous studies and minima in the power spectra (part 3.3) we chose to split our signal into the following bands of frequency: 65 to 120 days period (hereafter B65-120), 35 to 65 days period (B35-65), and 15 to 35 days period (B15-35). We also worked on a broader band including most intraseasonal frequencies from 25 to 90 days period (B25-90). Figure 2.3 shows the effect of this bandpassing on a time series of velocity. The sum of the three bands (B65-120, B35-65 and B15-35) is in good agreement with the raw series (seasonal and high frequencies excluded), except for some short events that were modified as shown by the arrows: two high frequencies events merged to produce a new fake event (this is seen mostly in B15-35).

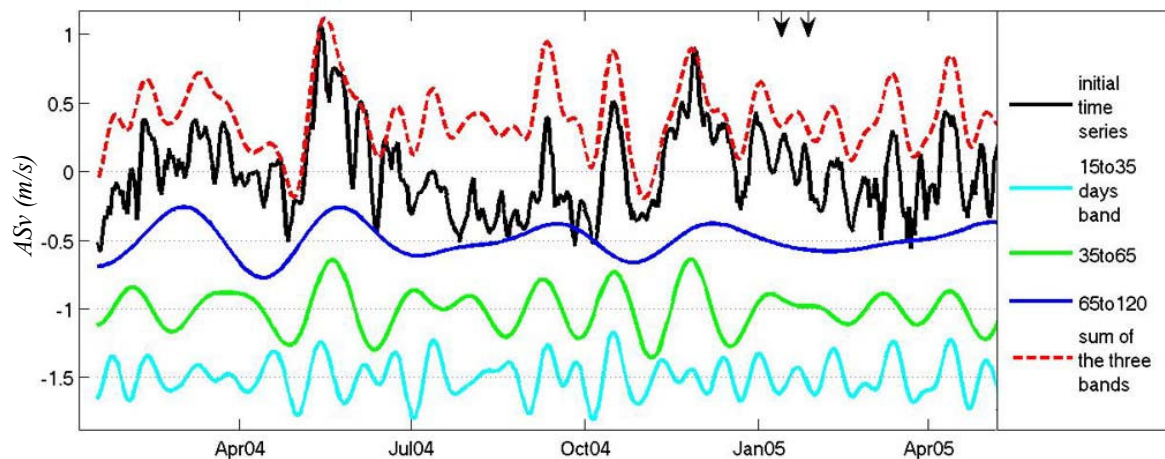


Fig 2.3 – Along Strait velocity at 100m depth in Lombok East and the bandpassed series

Method

We first worked with a method preserving the total variance using several low-pass filters. The principle of this method is to apply several different low-pass filters to the raw series and then subtract the results from it to obtain different bands of frequency. We didn't work with these results since the transition between the pass-band domain and the stop-band domain wasn't sharp enough due to shortness of our record.

The method we used is detailed as follows:

Given a starting time series $x(t_n)=x_n$ we will systematically convert the input $\{x_n\}$ into the output $\{y_n\}$. Because we work on prerecorded data we used a nonrecursive filter (where output value at one time is not taken into account to evaluate future output values). The output is obtained through the convolution:

$$y_n = \sum_{k=-M}^M h_k \cdot x_{n-k}$$

where h_k is the set of weights defining our filter and is the response to a spike-like impulse (see annex-4b). The length of the filter is $2M + 1$ it implies that we use $2M + 1$ points to evaluate the output at one date; to improve the definition of our filter we duplicated the time series by reflecting half the time series at the beginning and at the end; by this way we can apply a longer and more accurate filter.

The discrete Fourier transform of y_n is

$$\begin{aligned} Y(\omega) &= \sum_{n=-M}^M y_n \cdot e^{-i\omega_n \Delta t} \\ &= \sum_{k=-M}^M h_k \cdot e^{-i\omega_k \Delta t} \cdot \sum_{n=-M}^M x_{n-k} \cdot e^{-i\omega_{n-k} \Delta t} \\ &= H(\omega) \cdot X(\omega) \end{aligned}$$

The convolution in the time domain corresponds to multiplication in the frequency domain. Δt is our period of sampling, H is the admittance function or frequency response $H(\omega) = |H(\omega)| \cdot e^{i\phi(\omega)}$.

Once H is specified we find the weights by the inverse Fourier transform (see 3.3 **Method PSD**). $|H|$ is the gain; it has to equal 1 in the pass band $\omega_{c1} \leq |\omega| \leq \omega_{c2}$ and 0 in the stop bands (ideal filter). $\phi(\omega)$ is the phase lag, we want it to be zero everywhere, to avoid creating a phase shift in our bandpassed time series we applied the filter in one way and then in the reverse direction.

To sum up this operation: we define our desired transfer function in the frequency domain (see annex-4a), then we obtain the set of coefficients h_k of our filter by an inverse Fourier transform and finally we perform the convolution of our time series with this filter in the time domain.

As a test step of the efficiency of the method we tried these filters on fake time series, the conclusion of this study is that the method works very well to catch periodic sinusoidal shaped signal but when we try with a time series consisting only in short events coming back regularly we point out that the filtering produce inexistent signal in the short period; for this reason we didn't bandpass the wind time series but only subtracted the seasonal cycles.

2.5. Define a unique time base

Purpose

Allow further comparison between moorings

Now that the series only contain fluctuations with periods greater than 2 days we can decimate to suppress the redundant information. We chose to keep one value every 6 hours instead of the 30 minutes initial sampling rate; we also created time series on a one-day sampling to perform the correlation with the wind and time series on a one-week sampling (after applying a running mean filter) to perform the correlation with the sea level anomaly. The moorings were projected onto a common time base: same starting time, end time and sampling rate. Thus the period of the study starts on the 17th of January 2004 and ends on the 6th of June 2005.

Remark: when we have gaps in the time series at a given depth we linearly interpolate the blanks from the nearest points if the missing information doesn't represent more than 20% of the whole time span.

Conclusion

Before analysing the data and their physical meaning we need to be sure that we comment on significant features only and we need to prepare the data to facilitate further studies. Pre-processing data is thus of major importance for further results and interpretation.

3. The variability by mooring

Here we describe the basic statistics of the processed mooring data. In all part 3 we describe Lombok strait in detail and then comment other moorings in relation to Lombok.

3.1. Means, trends and variance

Purpose

Before estimating power spectra we detrend the time series to avoid errors at the very low frequencies. We also need to remove the mean of our series (especially temperature) if we want to compare the behaviour with depth. Here we describe these means and trends. The standard deviations of our time series is commented as an introduction to understanding the variability of the flow.

ASv

- Velocity mean is negative in all moorings (except Ombai North) at most of the depth except the very shallow depth which experience means close to zero, and the deep part of Timor Sill where the mean current is toward Indonesian seas (Eastward current). This mean velocity reflects the average flow of the Indonesian Throughflow (Fig 3.3a1); the magnitude of this mean velocity is around 0.2 to 0.4 m/s above 300m.

- No significant trends had been observed on the 16 months record.

- Standard deviation $\sigma = \left(\frac{1}{n} \sum_{i=1}^n (x_i - \bar{x})^2 \right)^{1/2}$

In Timor moorings the standard deviation is almost constant on the whole depth and increases slightly toward the surface from 0.1 to 0.14 m/s. In Ombai and Lombok West the standard deviation is greater and presents two distinct domains: the standard deviation is comprised between 0.15 and 0.25 m/s below 300m and between 0.3 and 0.5 m/s above; Ombai North mooring is the only one to present a maximum of variance around 175m and then a decrease toward the surface (see Fig 3.2). Lombok East shows a mix of these two descriptions with a very weak variability below 300m ($\sigma < 0.1$ m/s) and a strong increasing variability toward the surface.

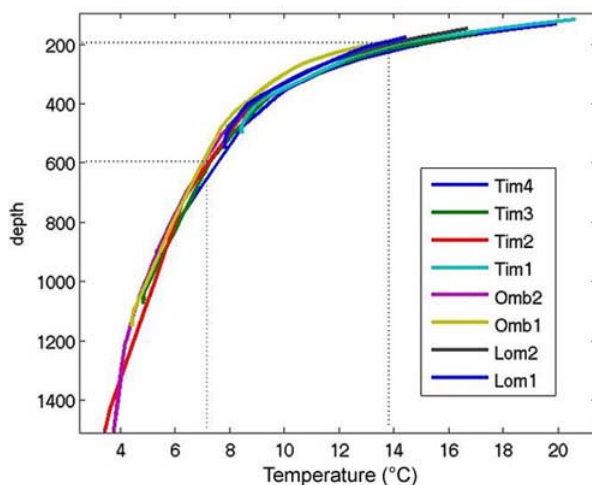


Fig 3.1 – Mean Temperature with depth in all moorings

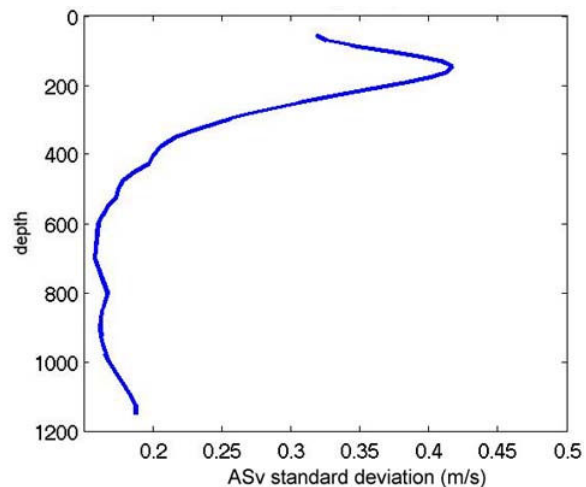


Fig 3.2 - Standard deviation of velocity with depth in Ombai North

(T)

- The mean temperature with depth is well scaled between moorings (Fig 3.1) and follows at each location the same shape: 14°C at 200m, 9°C at 400m, 7°C at 600m and 5°C at 1000m.
- No significant trends had been observed on the 16 months record.
- For temperature standard deviation we find again the opposition between Timor moorings and Ombai/Lombok. In Timor the standard deviation increases from 0.1 to 0.2°C below 600m and from 0.3 to 1°C between 400 and 100m. In Ombai and Lombok the standard deviation increases from 0.2 to 0.4°C below 600m and from 0.6 to 1.3°C between 400 and 100m.

(O) There are two periods in the year as regard the variability of temperature and velocity: from March to August the variables fluctuate more than from September to February and this especially in the short period variations, this is true especially in the southern moorings of Timor and could be related to the seasonal cycle amplitude.

A clearest picture of the variance is given in part 3.3: the frequency analysis giving a picture of the variance by frequency.

3.2. Temporal structure of the series

We work now with the detrended and mean-removed time series of temperature (T) and Along Strait velocity (ASv).

(ASv) The first thing we point out while looking at Lombok time series (see Fig 3.3 for an example) is the difference of behaviour with depth. The difference is made first between the 0-250m and the 250-500m layer where currents are much weaker (see 3.1 Variance with depth); second difference shows a decoupling between the variability of the 10-50m layer and the 50-250m layer: variations are not in phase (see part 3.4 for further details). Amplitude of variations can be more important in the latest layer, therefore some strong events (May 2004, November 2004...) can't be related to a local wind stress because the surface layer doesn't show the same response. Keeping in mind that the southern Lombok strait is at 280m depth, these two points bring us in looking for an Indian-side forcing.

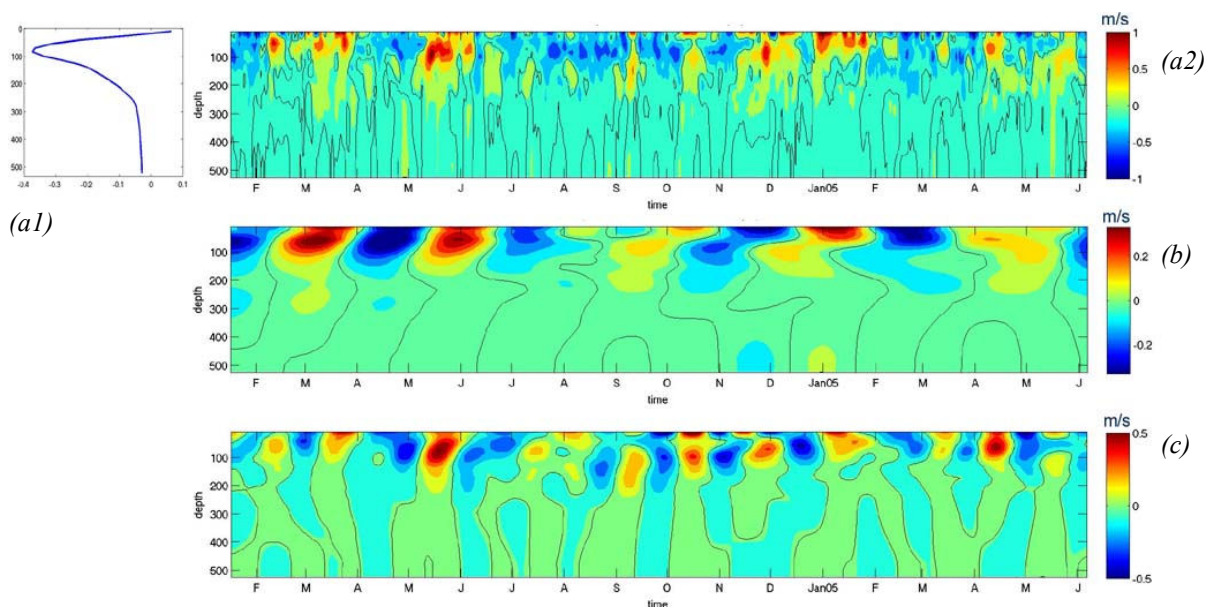


Fig 3.3 – Along Strait velocity with depth in Lombok East; (a1) mean ASv on the whole time span, (a2) raw time series, (b) 65-120 day band, (c) 25-90 day band.

Ombai and Timor Roti present a similar pattern. In Timor Sill, South Slope and Ashmore we only observe a difference between a surface layer (0-200m) and a deep layer, variability doesn't seem to be related between these two layer and the deep layer shows strong current especially in the sill.

T Temperature anomalies affect often the whole water column.

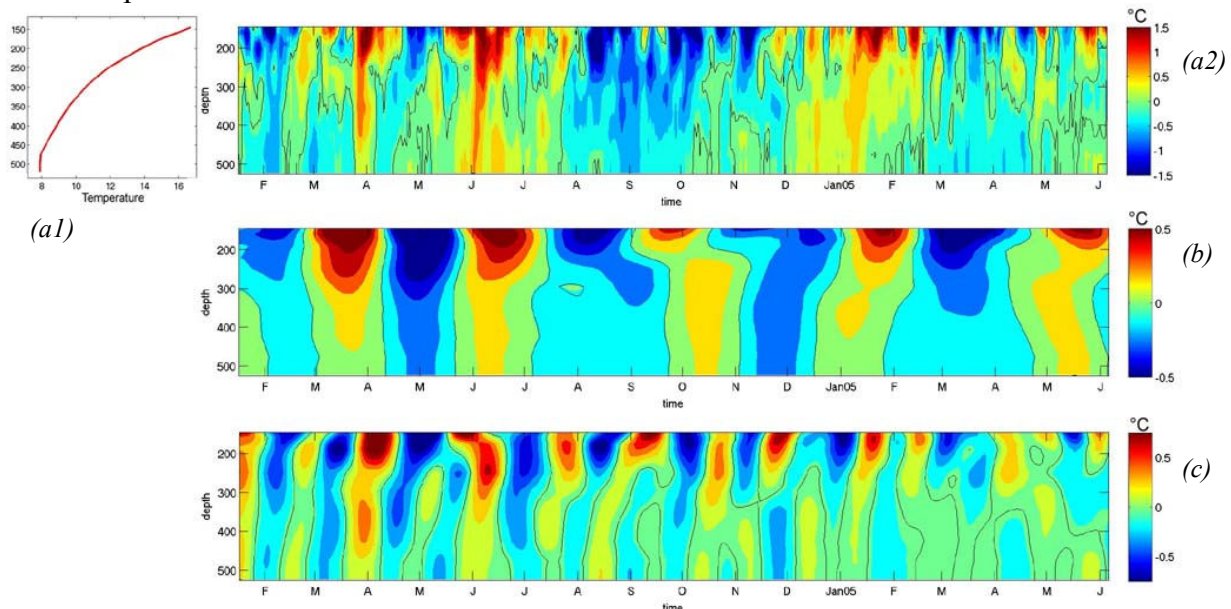


Fig 3.4 – Temperature with depth in Lombok East; (a1) mean T on the whole time span, (a2) raw time series, (b) 65-120 day band, (c) 25-90 day band.

O In both the velocity and temperature time series we point out that some isolated strong events account for a great part of the variability. Some of these events affect the whole depth while others affect only a given depth: around 100m for the March 2004 event in Lombok East velocity for instance.

When we filter the data the vertical structure of the anomalies appears. Most velocity and temperature anomalies show a vertical structure of propagation toward the surface while other anomalies are vertical. This feature is seen well in Ombai and Timor passages.

3.3. Frequency spectra: Power Spectral Density

We used the Power Spectral Density (PSD) to quantify the contribution of different frequencies to the total variance.

Method PSD

Power is defined as energy per unit time. For an integrable time series $y(t)$ the Fourier transform $Y(f)$ is

$$Y(f) = \int_{-\infty}^{+\infty} y(t).e^{-2i\pi ft} dt$$

If we want to find the time series with its Fourier transform as a starting point we use the inverse Fourier transform

$$y(t) = \frac{1}{2\pi} \int_{-\infty}^{+\infty} Y(f).e^{i\omega t} d\omega$$

The Energy Spectral Density is $S_E = |Y(f)|^2$. Division by dt of the ESD gives the PSD.

The Power Spectral Density is

$$S(f) = \int_{-\infty}^{+\infty} R_{yy}(\tau) \cdot e^{-2i\pi f\tau} d\tau$$

where $R_{yy}(\tau) = E(y(t) \cdot y(t + \tau))$ is the auto correlation function.

We used the periodogram method to compute the PSD.

All the plots of the power spectra were drawn as variance preserving spectra: plotting $S \cdot f$ versus $\ln(f)$. In this representation the area under the curve is equal to the amount of variance between the frequency boundaries.

$$Area = \int_{f_1}^{f_2} S(f) \cdot f \cdot d(\ln(f)) = \int_{f_1}^{f_2} S(f) \cdot f \cdot \frac{1}{f} df = \int_{f_1}^{f_2} S(f) \cdot df = Variance$$

We improved the reliability of our estimates by computing the spectral analysis on separate segments and then average the results but we lose precision in the spectral estimate.

ASv The spectrum of velocity in Lombok (see Fig 3.5 for an example in Lombok East) presents several maxima: around 15 to 20, 35 to 45 and around 70 to 90 days period band (B70-90); however the location of these picks has to be taken with care since the confidence levels are very wide. We confirm the observation of several different layers 0-50m layer presents a broad band of variability without distinct pick at one frequency; the 50-250m layer presents the maxima quoted above and the deep layer is quieter but still affected by high frequencies.

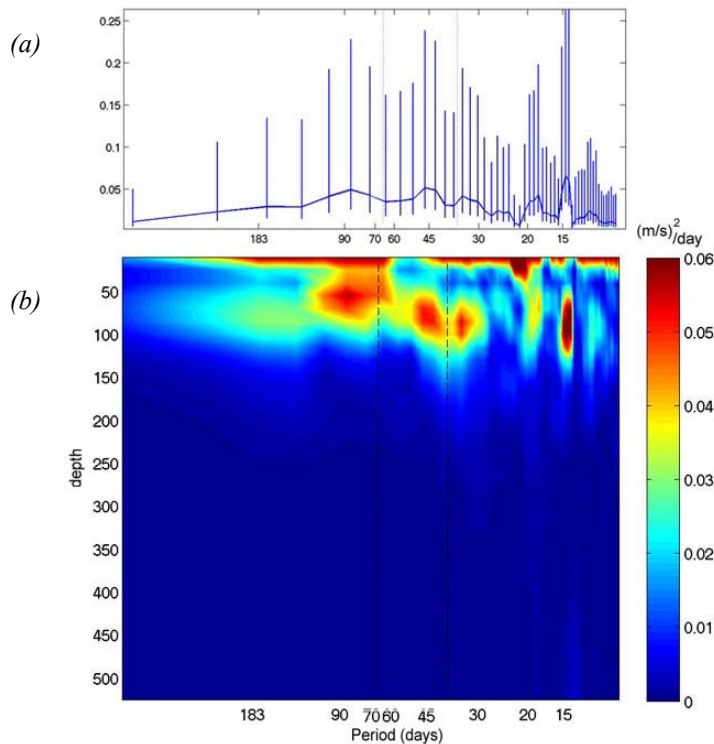


Fig 3.5 – Power spectral density (in $(m/s)^2/day$) of Along Strait velocity in Lombok East at one depth (70m) with 80% confidence levels (a) and at all depth (b)

Ombai North and Timor1 Roti velocity spectra show a remarkable picture because they are dominated by the high frequency variability: B10-45. Ombai South behaves almost as

Lombok in the B45-180 for the 100to900m depth layer; the spectrum is also characterised by a deep penetrating 15to40-day variability.

Timor2 Sill spectra is similar to Timor Roti one for the shallow layer (0-400m) but this mooring (the only one anchored in a sill) is remarkable for the strong deep (1400-1800m) variability around 30 and 50to90 day band.

Timor South moorings (Timor3 and Timor4) are characterised by a deep penetrating 30to40 day band and no energy in B70-90.

T The spectrum of temperature in Lombok presents maxima around 15, 20to30, 40to50 and 70to180 days period. Ombai North, Timor Roti, Ashmore, South Slope and shallow Timor Sill behave in a similar way.

Again in the Sill of Timor (1800m) we remark a strong variability of the temperature in B50-90.

3.4. Coherence spectra within each mooring

Purpose

In this part we analyse the correlation of the variables with depth to confirm the hypothesis saying that the different layers could be driven by different forcing and to confirm the observations of 3.1 on the vertical phase propagation of velocity and temperature anomalies.

Method Coherence

Given two time series $x_1(t)$ and $x_2(t)$ the coherence spectrum γ_{12}^2 is

$$\gamma_{12}^2(f_k) = \frac{|S_{12}(f_k)|^2}{S_{11}(f_k) \cdot S_{22}(f_k)}$$

where S_{12} is the cross spectrum such that $S_{12}(f_k) = \frac{1}{N\Delta t} X_1^*(f_k) \cdot X_2(f_k)$ and S_{xx} and X_i are defined in 3.3. Here $\gamma_{12}(f_k) = |\gamma_{12}^2(f_k)|^{1/2} e^{-i\phi_{12}(f_k)}$ where $\phi_{12}(f_k)$ is the phase lag between the two signals at the frequency f_k .

In all the figures of coherency, we plot γ_{12}^2 which represents the fraction of variance shared between x_1 and x_2 and $\phi_{12}(f_k)$ which allows to find out the phase shift (or time lag $\Delta t = \Delta\phi/\omega$) existing between two time series, this will be useful to identify propagating phenomena. We have to keep in mind that coherence is highly dependent on noise in our time series.

We compute the coherence of the variables between one depth and the same variable at all other depths within each mooring to know how well the variables are correlated within the water column.

T The first thing to point out is the relationship between the deepness of the coherent water column and the frequency. At low frequency (B60-250) the water column is fairly coherent on a large scale whereas at high frequency the coherence is lost very quickly on the vertical (see annex-5). This characteristic is seen mostly in temperature spectra and to a lesser extent in velocity. Low frequency coherence is systematically associated with upward phase propagation.

The largest coherent layers are always found in the deep part of the moorings.

Some frequencies make an exception to this first picture and coherence can be seen on a larger layer. Often B30-40 variability of Temperature (and Velocity) shows a large coherence with depth (seen in Ombai, Timor South Slope and Ashmore in the deep part). This coherence is associated with an upward phase propagation.

ASv In Lombok there is a striking feature of correlation: velocity is fairly coherent within the upper layer (50-300m) and within the 300-500m one but there is no correlation between both layers (Fig 3.6). This is true especially for velocity while temperature on long period variability is more coherent with depth. The same can be said for velocity in Timor, the strong decoherence layer being around 200m: the upper layer is completely decorelated from everything happening below. Again some frequencies show coherence on a larger depth: around 20, 35 and 50 day band. Velocity in Ombai South is largely coherent with depth in B30-35.

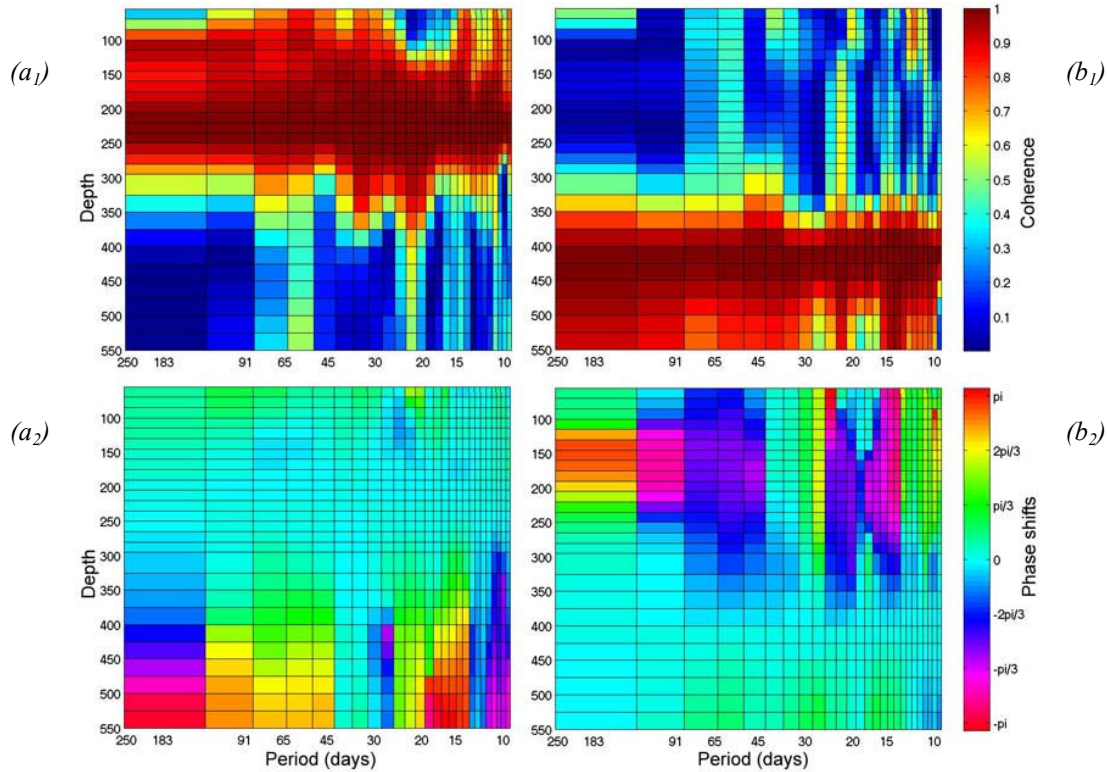


Fig 3.6 – Coherence of velocity with depth in Lombok West taking as the reference 220m depth (a₁) and 400m depth (b₁) associated with the phase shift (a₂) and (b₂).

o We also performed the coherence between Along Strait velocity and Temperature depth by depth to check if some bad behaviour associated with the moorings motion remained in the data. Indeed when the line is pulled down by a strong current, temperature sensors experience a colder temperature, if we didn't correct well this effect we expect to have a strong anti-correlation between the two variables.

No coherence is observed between ASv and T in Timor1, Timor3 and Timor4. In Lombok and Ombai moorings we observe only one patch of high coherence in B80-180 associated with a $-2\pi/3$ phase shift.

Timor Sill coherence spectra however presents a strong relation between ASv and T in B60-120 below 800m. This coherence is associated with a phase shift of $\pm\pi$. Given that the motion of the mooring is more important in the shallow water and this coherence is only seen in the deep part of the mooring, the hypothesis of a motion linked effect has to be rejected.

One hypothesis we can propose is that temperature variations create currents in this deep part of Timor Sill; this hypothesis will be further discussed in 5.1.2.

Conclusion

The behaviour of the variables varies with depth. The upper layer experience stronger variability which account for an atmospheric influence. Several forcings seem to drive the variability since various layers behave distinctly and fluctuations are not in phase.

We have to keep in mind that spectral analysis presupposes a periodic behaviour in the time series, however variability in our time series is often supported by isolated strong events.

Visual inspection and coherence analysis show a vertical phase propagation of most events reversing the flow. This vertical phase propagation toward the surface is characteristic of the downward propagation of energy associated with Kelvin waves propagation (and gravity waves in general).

4. The variability in the region

4.1. Comparing the series between moorings

We plot the time series of Temperature and Velocity of all moorings record on the same plot to have a first visual inspection of the common behaviour of the variables within the whole region.

ASV Because the amplitude of variations is different in each strait, Fig 4.1 shows the normalized Along-Strait velocity at 250m. Some strong events can be followed between moorings. Timor and Lombok/Ombai form two distinct groups within which we find common events. Downward arrows highlight events found in both Lombok and Ombai records and upward arrows stand for Timor ones. In Timor the period from February to July 2004 shows common behaviour between moorings while it is less evident during the last part of the year; in this period we point both events appearing first in the northern part τ_1 and some appearing first in the southern τ_2 . In Lombok and Ombai moorings common strong events appear evidently correlated in the layer around 100m and Lombok events are leading Ombai ones.

T Temperature in each strait appears strongly correlated between moorings however northern part and southern part of Timor doesn't appear to follow the same forcings. Few strong events can be followed between straits.

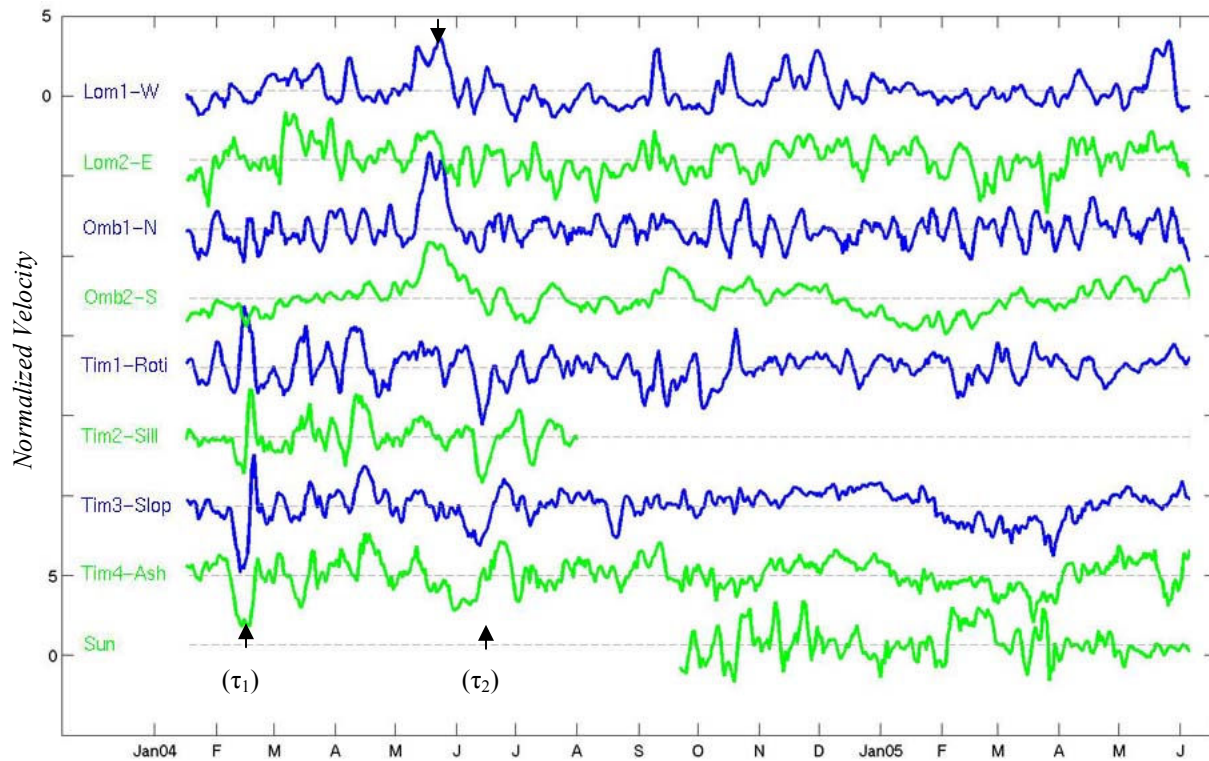


Fig 4.1 – Normalized ASv in each mooring at 250m

4.2. Coherence between moorings

Purpose

Here is described the coherence of variables at the same depth between moorings using the definition of coherence of part 3.4. The purpose of this study is to track common behaviour of the variability between straits.

ASV Only the upper part of velocity is coherent between Lombok East and West (0-350m for lower frequencies in B50-180 and 0-200m in B10-50) with a lag close to zero. Ombai South shows a good coherence with Lombok on the 0-250m layer in B30-120. Variability in Lombok leads Ombai South with a 5 to 10 days lag (see Fig 4.2).

Timor moorings show no coherence with Lombok. No coherence is seen either between Ombai and Timor except between deep velocity in Ombai South and Timor Sill in B50-180 with Ombai leading by 5 to 10 days (this result has to be taken with care since the time span of the common records is short). Ombai North is not coherent with the velocity anywhere excepted in B35-65 / 100-300m layer with Lombok (5 days lag delay).

Within Timor passage, velocity in Roti and Timor Sill are coherent in the 100-300m layer at all frequencies with a near-zero lag. Ashmore and South Slope are coherent only in the low frequency band with no lag. These two details excepted Timor Velocities are inconsistent between moorings. In Timor the picture is not clear as regard the direction of propagation of the events (see 4.1), and only one period of the year seems to show a common behaviour; these could explain the poor statistical coherence observed here.

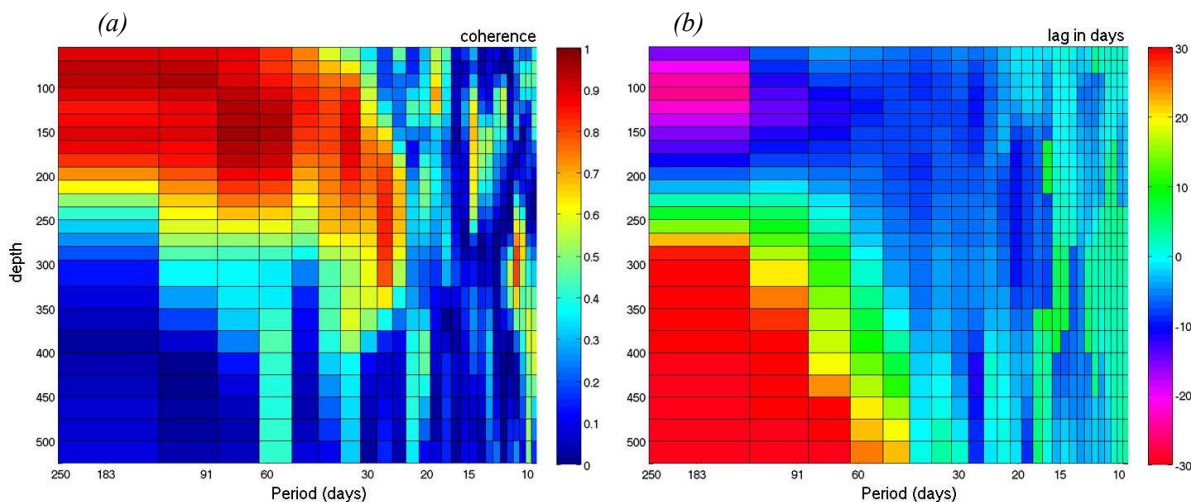


Fig 4.2 – Coherence between Ombai South and Lombok West velocity (a); associated temporal lag (b) (Lombok being the reference a negative lag means that Lombok is leading)

T Within Lombok moorings or within Ombai ones the coherence is high in B25-180 on the whole water column with no lag, thus both side of these straits experience the same temperature variability. When it comes to comparing Temperature between straits we cannot observe any coherence.

Conclusion

Variability of the flow in Lombok and Ombai is partly coherent. Lombok events in B30-120 are leading Ombai ones by 5 to 10 days. This is an argument to imagine a common forcing being responsible for the variability and propagating between these two straits.

The situation in Timor passage appears less clear since no coherence is observed with Lombok or Ombai variability. Even within Timor moorings coherence is poor, this could be due to several local forcings being responsible for the variability in the region.

Coherence between moorings was computed on a depth-to-depth-basis: we correlated variables at each depth of one mooring with the same depth of another mooring. An isodensity-basis comparison may be preferable but requires information not available in this study.

5. Origin of the variability

Atmospheric forcings are now studied in relation to the variables in the straits to figure out the place of the variability observed in response to local and remote forcings.

How do the variables in the straits vary?

One forcing of velocity in the ocean is the creation of a pressure gradient either by a modification of the sea level or in a lesser extent by internal density modification. Indeed when the sea level varies at one side of the strait, it creates an along strait pressure gradient which affects the velocity: the current is modified and balanced by the frictional terms (friction at the bottom and on the sides). A cross strait gradient can go along with this sea level anomaly and affect the velocity by the geostrophic balance^[1].

A westerly wind burst could on top of the current pattern determination be responsible for the emission of Rossby and Kelvin waves by creating a pressure gradient^[7] that is why we want now to test this hypothesis: *The origin of these sea level variations may be imputed among other to Kelvin waves (definition 5.2) propagating from the Indian Ocean and created by wind forcing.*

Kelvin waves also have a consequence on temperature associated with propagating vertical displacement of the thermocline.

5.1. Spatial correlation with the wind stress

Data

We used remotely sensed surface wind data from ERSs who provides synoptic gridded fields of wind parameters retrieved from NASA scatterometer SeaWinds onboard QuikSCAT.

The sensor measures backscattered microwave signal, but since the atmospheric motion doesn't affect significantly these wavelength, the wind stress over the ocean is evaluated from the roughness of the surface. The wind stress on the ocean creates ripples and waves modifying the roughness and hence the backscatter signal, however the relation giving the wind speed from this signal measured is not known theoretically and is evaluated by empirical inversion algorithms. To estimate surface wind stress, for each scatterometer wind vector, the following bulk formulation is used: $\vec{\tau} = \rho C_D \vec{v}$ where ρ is the density of the air, C_D the drag coefficient and \vec{v} the wind vector at 10m above the surface.

Method Lagged Correlation

The lagged covariance C_{ab} between velocity or temperature (x_a) and wind stress or sea level anomaly (x_b) is computed as follow (the mean value of all time series are removed prior to the computation).

$$C_{ab}(\tau) = \frac{1}{N-m} \sum_{n=1}^{N-m} x_a(n\Delta t) \cdot x_b(n\Delta t + \tau)$$

Where N is the total number of point in the series, $\tau = m\Delta t$.

In all the figures of the 5th part correlations were normalized so that the auto-correlations at lag zero equal one, all following figures draw $\rho_{ab}(\tau)$

$$\rho_{ab}(\tau) = \frac{C_{ab}(\tau)}{[C_{aa}(0) \cdot C_{bb}(0)]^{1/2}}$$

5.1.1. Correlation between wind stress and variables at one depth

ASv Lag correlation with the along strait current at one depth

We correlate the wind stress in each box of ½ degree with the along strait current around 100m (bandpassed as explained in 2.4.2) to have a first idea of the geographic importance of wind forcing on currents in the straits. Annual and semi-annual cycles were suppressed in the wind stress time series (part 2.4.1).

Lagged correlation between zonal or meridional wind stress and velocity in all frequency bands were plotted and analysed; the main results of the analysis of these figures are the following:

- In Ombai and Timor Roti (and to a lesser extent in Lombok) the velocity shows a correlation with the **local zonal wind stress** over Flores and Banda seas and the southern Sawu sea. This can be seen best in the high frequency band (15 to 35 days period). A positive correlation with the zonal wind stress exists with a maximum for 4 (Ombai) to 8 (Roti) days leading of the wind, and a negative correlation exists with the meridional wind stress at the same lags. In other words an eastward or southward wind burst leads to a reverse of the Throughflow. This correlation suggest an Ekman effect which tends to create a current to the left (in the southern hemisphere) of the wind stress.
- In Lombok and Ombai the **influence of the Indian Ocean** is predominant. Zonal wind stress around the equator in the central and eastern basin shows a positive correlation with the current 15 (in Lombok) to 20 (in Ombai) days later (Fig 5.1). This feature is seen especially in B25-90. This correlation is supported mainly by eastward wind stress bursts which trigger a reverse of the flow two to three weeks later in the straits (see 5.2 for an example).

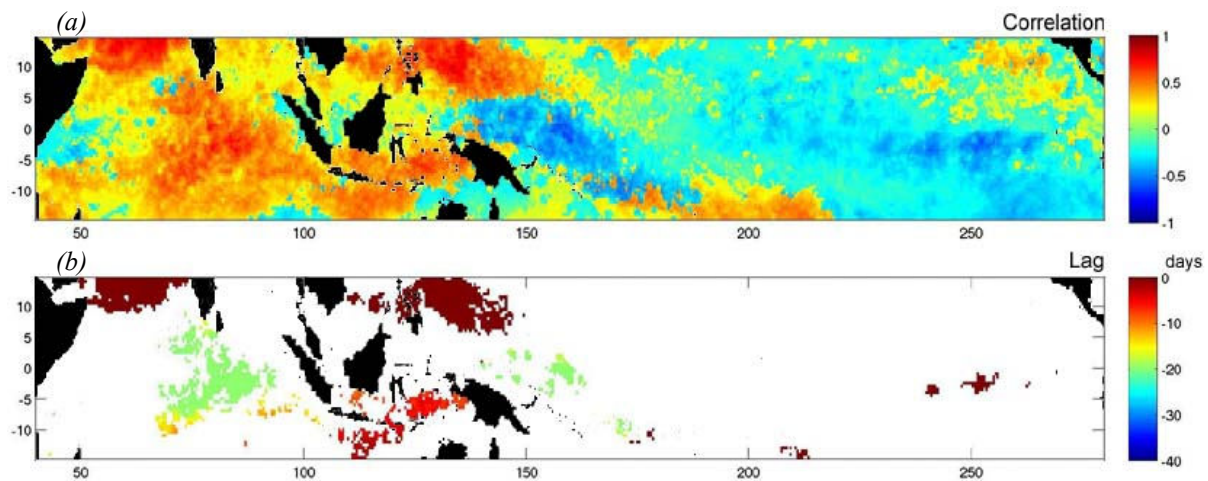


Fig 5.1 – Map of maximum correlation (among all lags) between zonal wind stress and ASv in Ombai South in B25-90. The maximum correlation (a) and corresponding time lags τ (only for correlation greater than 0.5) (b) are shown.

- In Lombok East and Ombai we observe a negative correlation with the *meridional* wind stress along the equatorial Sumatra coast at a lag of 10 to 15 days. A southward wind is followed by a north-eastward current some days later. This could be interpreted as an effect of the Ekman current induced by the wind near the coast: southward wind piles water toward the coast (and creates downwelling conditions); the sea level anomaly could propagate as a coastal Kelvin wave and produce an along strait pressure gradient reversing the flow.

T Lag correlation with the temperature at one depth

Using the method presented above, correlation between wind stress and temperature (between 250 and 300m) can be commented as follow:

- Only Ombai North and Timor South (Ashmore and South Slope) show a correlation between the local wind forcing and temperature. In Timor the correlation is negative with the zonal wind stress leading by 1 to 5 days. Again this observation could be related to an Ekman effect. For instance an eastward wind stress may trigger a northward upwelling favorable current in the southern slope of Timor. The correlation in Ombai North is positive and the same hypothesis can explain the observation because this mooring is situated on the southern shore of Flores islands.

- In Lombok, Ombai and to a lesser extent Timor Roti the temperature is correlated to East Indian and along Sumatra/Java coast wind forcing. The correlation is positive with the zonal wind stress on central to eastern Indian Ocean and negative with the meridional wind stress off Sumatra (positive wind toward the North). We observe a progression in the lag of the wind leading: central Indian Ocean leads the temperature by around 15 days in Lombok, 20 days in Ombai South and 25 days in Timor Roti; Sumatra coast wind stress leads the temperature by 10 to 15 days in Lombok, 15 to 20 days in Ombai and 20 to 25 days in Roti. These correlations may be explained by the same origin as the velocity anomalies discussed above.

- No influence of the Pacific side was seen in temperature.

Remark: Variables in Ombai North are more locally driven as regard the wind forcing whereas Ombai South shows more correlation with Indian Ocean forcing. We could explain this difference remarking that Ombai South is situated in the core of the Throughflow.

5.1.2. Correlation between variables at all depth and wind indexes

Because the wind variability is very broad scale as we saw just before, we can sum up this information by picking some region in which we average the zonal or along coast wind stress (Fig 5.2). The regions are chosen taking into consideration the shapes of the correlation given in 5.1.1; all indexes are taken positive for an eastward wind stress.

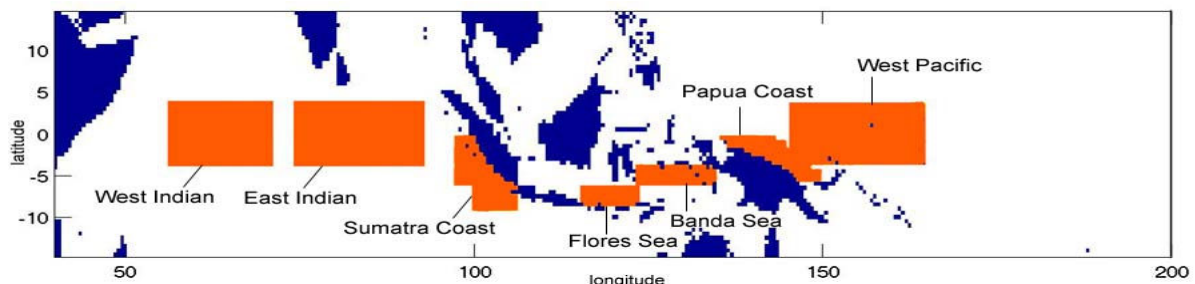


Fig 5.2 – Regions defining our indexes of wind

We chose three regions to study the Indian influence: West Indian, East Indian where we only keep the zonal wind stress and the Sumatra coast where we average the along coast wind stress. For the local Indonesian seas influence we worked with a Flores sea index just north of the Lombok and Ombai moorings and with Banda Sea index further north-east; in these regions we only take into account the zonal wind stress. For the Pacific influence we kept a West Pacific index (equatorial zonal wind stress) and an along coast wind stress north of Papua.

Preliminary checking:

To check the representativeness of our indexes we correlate them with the wind stress everywhere.

The Flores index appears highly correlated to the Flores and Sawu seas zonal wind stress (north and south of the Flores archipelago). It is also correlated negatively to the meridional wind stress over the Banda Sea. The Banda index is fairly correlated to the zonal wind stress over Flores Sea and shows the same correlation with the meridional wind stress over the Banda Sea. Thus both these indexes take into account a common part of information and will be commented together.

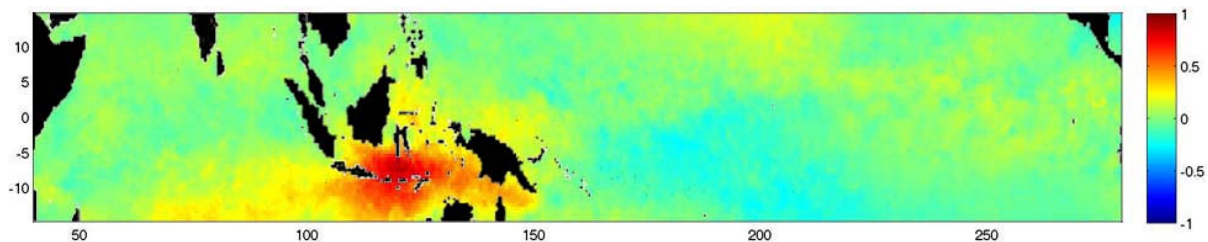


Fig 5.3 – Correlation between zonal wind stress and Flores Sea index

East Indian index is very locally correlated with the zonal wind stress but also shows a negative correlation with the meridional wind stress off Sumatra, it is thus a good index to comment on in relation to Sumatra one which take into account information further south.

Pacific indexes are very locally correlated as regard the zonal wind stress.

Now with these indexes describing the wind variability we calculate the lagged correlation with both variables at all depth in each mooring. Current and Temperature time series only contain the intraseasonal band B25-90; the wind wasn't bandpassed but we subtracted the annual and semi-annual cycles (as explained in 2.4). These correlations were computed with a lag introduced in the mooring time series, thus a negative lag signifies that the wind is leading.

Indian wind stress forcing (latitude: -4 to +4; longitude: 74 to 93)

ASV The correlation of the wind stress over the eastern part of the basin and the velocity in Lombok is maximum for a 14 days leading (Fig 5.4). A positive correlation signify that an Eastward wind is correlated with a Northward current 14 days later. The correlation affects the 80-300m layer at a progressive lag toward the surface (the maximum correlation follows a linear trend with depth: 12 days lead at 240m and 15 days at 100m...), we point out that the correlation doesn't affect the surface layer (0 to 80m depth).

In Ombai, the same wind index shows a correlation with the 100-700m depth layer with a lag progressing toward the surface (15 days at 600m and 21 days at 200m). Around 800m exists a strong cut off in the behaviour of the correlation and below 1000m a correlation exists at a 40 days lag.

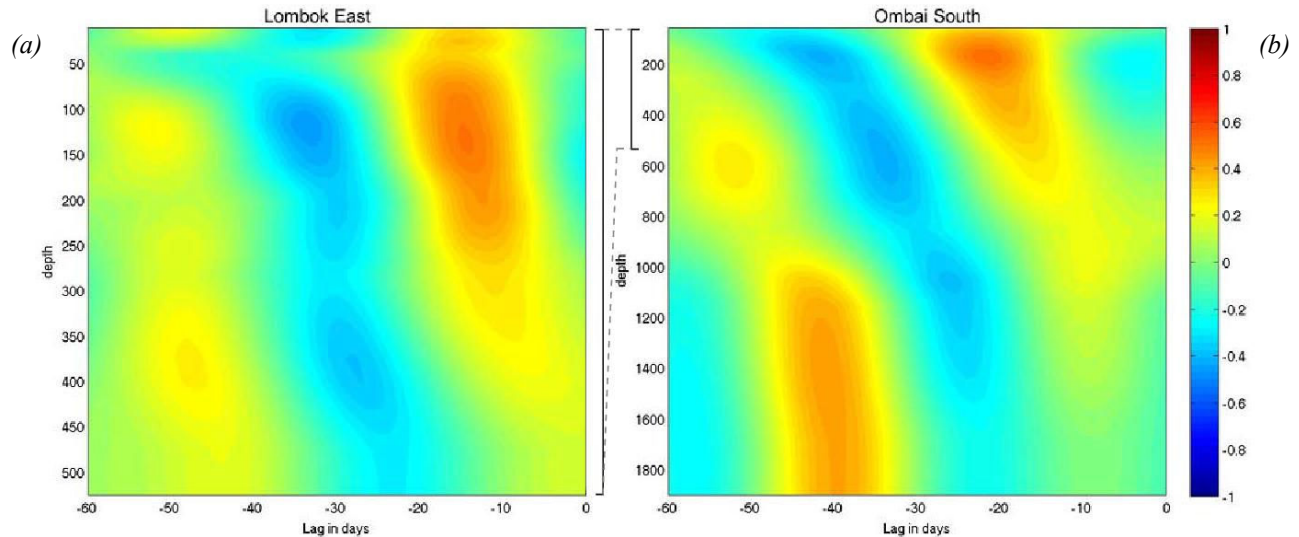


Fig 5.4 – Lagged Correlation between the zonal wind stress index on Eastern equatorial Indian Ocean and Along Strait velocity in Lombok East (a) and Ombai South (b)

Finally the only reasonable correlation in Timor passage related to the wind forcing in this region (here with the along Sumatra coast wind stress) is observed in Timor Sill and affects only the layer below 900m. The correlation is negative and the lag corresponding to the maximum is between 10 to 14 days (Fig 5.5a).

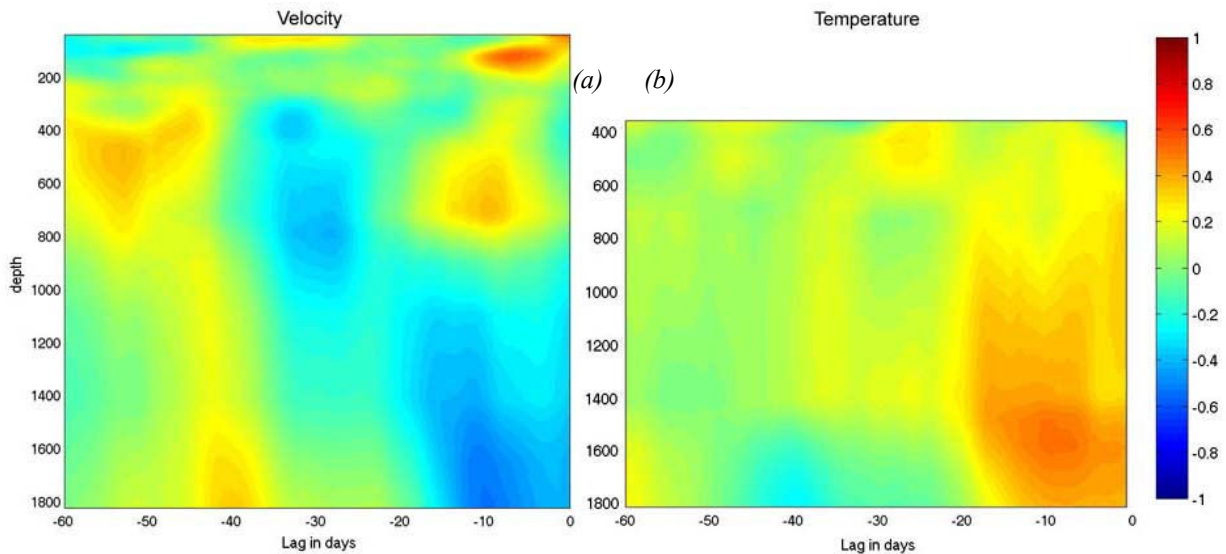


Fig 5.5 - Lagged Correlation between the zonal wind stress index along Sumatra coast and Along Strait velocity (a) and Temperature (b) in Timor Sill

T The temperature response to East Indian wind stress in Ombai shows the same structure as the velocity response with a slightly longer lag (one or two days). We point out the transition of behavior around 900m where the main correlation feature vanishes. The temperature response to East Indian wind stress in Timor Sill shows the same structure as the velocity response at the same lag but with a positive correlation (Fig 5.5b).

H Hypothesis:

- How to understand the correlation observed?

An eastward wind stress over East Indian Ocean is followed by an almost northward current anomaly in Lombok (almost eastward in Ombai) 15 to 20 days later which means a reversal

or weakening of the mean flow; this velocity anomaly go along with a positive temperature anomaly.

An equatorial then coastal Kelvin wave could carry a velocity and pressure anomaly on the Indian side of the strait resulting in the reversing of the main flow^[3]. This pattern is downwelling favorable off Sumatra and a positive temperature anomaly is thus propagating along with the velocity one.

- How to interpret the vertical progression of time leading?

A wave with an upward propagating phase would create an anomaly of temperature or velocity showing this pattern.

- How to interpret the vertical structure of the correlation?

Indian Ocean wind seems to affect the current in the 100-300m layer in Lombok roughly, it could be explained by the fact that the first 80m layer is more influenced by local wind forcing over Flores and Banda seas, and the southern strait of Lombok does not allow the waves to influence the variables deeper than the sill (around 300m).

Ombai is very similar to Lombok in the correlation observed although the depth of the layer affected is greater (100-700m). The longer time leading (20 days) could be explained by the traveling time of the wave along the south Flores island coast pathway. This pathway presents a sill around 800m north of Sumba island.

Correlation in Timor shows a deep negative correlation. One hypothesis we could put forward is that positive south-eastward wind stress along the Sumatra-Java coast being downwelling favourable, the warm anomaly propagates to Timor (by the southern coast of Sumba pathway) and places less dense water on the Indian side causing a negative (westward) current in the sill. This hypothesis would confirm the results of coherence previously observed: a strong anti correlation exists between velocity and temperature in the deep part of Timor especially for long period variability.

Indonesian wind stress forcing

ASV The Flores Sea is just North of the Flores islands between Lombok and Ombai straits. The correlation of the zonal wind stress here with current shows an influence mostly in the shallow layer above 80m. Both Lombok and Ombai South moorings are affected. The corresponding lag of 4 days argues for an Ekman effect being responsible of this response. We point out that Flores index is highly correlated to zonal wind stress over the Sumba Sea, thus the local effect is indifferently driven by wind stress north and south of Flores archipelago.

In Timor, only the two southern straits show a correlation with the wind stress over Banda Sea. Maximum correlation lag evolves from 14 days at 1000m to 22 days at 300m and no correlation is observed above.

T Temperature responses to the Indonesian seas wind stress forcing does not show significant correlations.

West Pacific wind stress forcing (latitude: -4 +4; longitude: 145 165)

Wind stress over this region shows very few correlations with the velocity and temperature in the straits.

Sea Level Anomaly (SLA)

The same study (as presented in part 5.1) was performed on SLA to confirm the mechanism connecting wind stress and velocity anomalies in the straits. Presentation of the whole study is not necessary in this report but some results may be exposed. Correlations between variables in the straits and SLA were weak. However SLA off Sumatra/Java coast shows clear correlation with Temperature in Lombok (resp Ombai) on the 50-250m layer (resp 50-700m) with one week leading (resp two weeks). Again a cut off is observed around the depth of Lombok Sill (resp Sumba Sill).

5.2. The 'May-2004 Event'

Purpose

Intraseasonal variability of the flow is mainly constituted by strong reversing events. This part describe one of these events to understand the mechanisms leading to a reversing of the ITF.

5.2.1. Description of the Event

On the 28th of April 2004 an eastward zonal wind stress anomaly begins to build on the equator on central Indian Ocean (lat: -5 +2 / lon: 80 90 E). It remains here until the 5th of May with the climax on the 2nd of May (Fig 5.6a).

A positive Sea Level Anomaly centered on the equator in East Indian Ocean (lon: 90 100 E) appears on the 5th of May spreads along all Sumatra Coast around the 12 (Fig 5.6b) and further south along Java coast around the 19 before vanishing in early June emitting two Rossby waves westward at $\pm 4^\circ$ latitude.

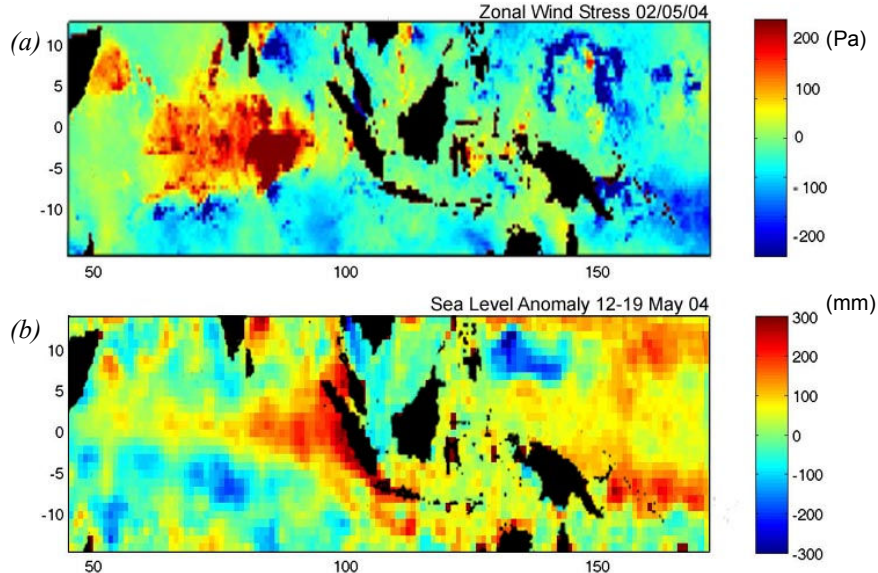


Fig 5.6 – Pictures of Zonal Wind Stress (a) and Sea Level Anomaly (b) fields illustrating the initiation of the May-2004 Event

ASV In Lombok and Ombai straits several of the biggest events reversing the flow occur during this event. Two major events are seen in Lombok: on the 14th and 24th of May (Fig 5.7); a smaller one on early June (on the 6th). In Ombai North two events can be described around the 20th and 25th of May while in Ombai South only one long event is observed around the 26th of May (Fig 5.7). No strong velocity anomalies are seen in Timor moorings.

(T) This period shows also strong warm events. In Lombok three picks can be separated: on the 26th of May, on the 6th and on the 19th of June. They affect mostly the 250 first meter but the 6th June event also affect to a lesser extent the deeper part. In Ombai the temperature anomaly span almost two weeks around the 28th of May.

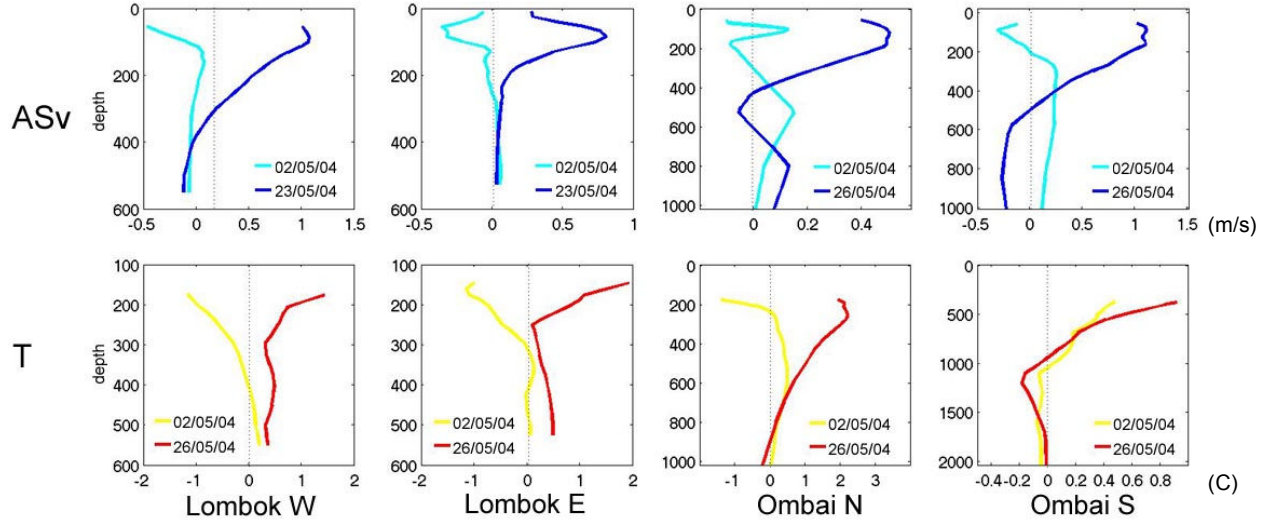


Fig 5.7 – Along Strait Velocity and Temperature anomaly in the two straits affected by the event; the figures represent the situation with depth during the strongest part of the event and the situation on the 2nd of May is given as an example for comparison

5.2.2. Physics

Here we describe the simplest model in which the Kelvin waves mentioned above appear.

5.2.2.a. Shallow water model equations on a sphere

The simplest model to describe the Kelvin waves is the shallow water model applied to a beta plane; it is important to take into account the Earth's curvature especially when dealing with low frequencies. In the approximation of the beta plane Coriolis parameter $f = \beta \cdot y$ where y is the distance to the equator, this approximation gives good result in our region of interest.

(O) Equations for the horizontal motion are

$$\frac{Du}{Dt} - \left(2\Omega + \frac{u}{r \cos \varphi} \right) \cdot v \sin \varphi = - \frac{1}{\rho r \cos \varphi} \frac{\partial P}{\partial \lambda} \quad (5.2.1)$$

$$\frac{Dv}{Dt} - \left(2\Omega + \frac{u}{r \cos \varphi} \right) \cdot u \sin \varphi = - \frac{1}{\rho r} \frac{\partial P}{\partial \varphi} \quad (5.2.2)$$

and the continuity equation is

$$\frac{\partial \eta}{\partial t} + \frac{1}{r \cos \varphi} \left[\frac{\partial}{\partial \lambda} ((H + \eta)u) + \frac{\partial}{\partial \varphi} ((H + \eta)v \cos \varphi) \right] = 0 \quad (5.2.3)$$

where r is the radial coordinate, φ is the latitude, λ is the longitude and

$\frac{D}{Dt} \circ = \frac{DH}{Dt} \circ = \frac{\partial}{\partial t} \circ + \frac{u}{r \cos \varphi} \frac{\partial}{\partial \lambda} \circ + \frac{v}{r} \frac{\partial}{\partial \varphi} \circ$. We also have $P = \rho \cdot g \cdot \eta$ in the shallow water model.

These equations describe the equilibrium between acceleration, Coriolis acceleration and pressure gradient.

◉ We are now looking for the solutions of small perturbation to a rest state $u=u_0+u'$, $v=v_0+v'$ and $\eta = \eta_0 + \eta'$. (5.2.1)-(5.2.3) become

$$\partial_t u - 2\Omega \sin \varphi \cdot v = \frac{1}{r \cos \varphi} g \frac{\partial \eta}{\partial \lambda} \quad (5.2.4)$$

$$\partial_t v + 2\Omega \sin \varphi \cdot u = \frac{1}{r} g \frac{\partial \eta}{\partial \varphi} \quad (5.2.5)$$

$$r \cos \varphi \frac{\partial \eta}{\partial t} + \frac{\partial(Hu)}{\partial \lambda} + \frac{\partial(Hv \cos \varphi)}{\partial \varphi} = 0 \quad (5.2.6)$$

To find the differential form of the equation describing gravity waves we take the divergence of 5.2.4 and 5.2.5 and substitute from 5.2.6

$$\frac{\partial^2 \eta}{\partial t^2} - c^2 \Delta \eta + fH\zeta - \beta Hu = 0 \quad (5.2.7)$$

Where $c^2=gH$, $f = 2\Omega \sin \varphi$, $\beta = \frac{1}{r} \frac{\partial f}{\partial \varphi} = \frac{2\Omega \cos \varphi}{r}$, $\zeta = \frac{1}{r \cos \varphi} \left(\frac{\partial v}{\partial \lambda} - \frac{\partial(u \cos \varphi)}{\partial \varphi} \right)$ is the vertical component of the vorticity and $\Delta^\circ = \Delta_H^\circ = \frac{1}{r^2 \cos^2 \varphi} \frac{\partial^2}{\partial \lambda^2} + \frac{1}{r^2 \cos \varphi} \frac{\partial}{\partial \varphi} \left(\cos \varphi \frac{\partial}{\partial \varphi} \right)$ is the Laplacian.

◉ Because we only consider phenomena close to the equator, we can simplify our equations remarking that: $\sin \varphi \approx \varphi$, $\cos \varphi \approx 1$, $\beta = 2\Omega / r$ ($= 2,3 \cdot 10^{-11} m^{-1} s^{-1}$) and $f = \beta \cdot y$. Under these approximations the model becomes

$$\partial_t u - \beta y v = -g \partial_x \eta + X / \rho H \quad (5.2.8)$$

$$\partial_t v + \beta y u = -g \partial_y \eta + Y / \rho H \quad (5.2.9)$$

$$\partial_t \eta + \partial_x (Hu) + \partial_y (Hv) = 0 - E / \rho \quad (5.2.10)$$

X , Y and E are external forcing, we can see X and Y as surface stress and E as an evaporation rate changing the properties of the layer; here $\zeta = \partial_x v - \partial_y u$.

5.2.2.b. Equatorial Kelvin wave

“The equatorial zone acts as a waveguide that is to say disturbances are trapped in its vicinity”^[6] and the motion is unidirectional, parallel to the equator. Under these conditions 5.2.8 and 5.2.10 become

$$\partial_t u = -g \partial_x \eta \quad (5.2.11)$$

$$\partial_t \eta + H \partial_x (u) = 0 \quad (5.2.12)$$

The solution for each variable is the sum of two non dispersive waves travelling in opposite direction. Keeping only the solution that decays exponentially with the distance to the equator the complete solution wave is

$$\eta = e^{-y/a_e} \cdot G(x - ct) \quad (5.2.13)$$

$$u = g/c \cdot e^{-y/a_e} \cdot G(x - ct) \quad (5.2.14)$$

$$v = 0 \quad (5.2.15)$$

Where $a_e = \sqrt{c/2\beta}$, G has the form of the forcing (wind stress); if we imagine it as a sinusoidal function (we saw that this description is not perfectly realistic) the solution is:

$$\eta = \eta_0 e^{-y/a_e} \cdot \cos(kx - \omega t) \quad (5.2.16)$$

$$u = \sqrt{g/H} \eta_0 e^{-y/a_e} \cdot \cos(kx - \omega t) \quad (5.2.17)$$

When an equatorial Kelvin wave propagates toward a land, it produces coastal Kelvin waves propagating with the coast on its left.

Comments:

Amplitude decays from the equator or from the coast with a distance of order a_e the equatorial radius of deformation.

The equatorial Kelvin wave propagate Eastward without dispersion following the relation $\omega = kc$ where k is the east-west wave number. Both phase velocity and group velocity propagate eastward. H is seen as the total depth when dealing with barotropic waves and as the equivalent depth for baroclinic ones.

For the first baroclinic wave mode in the ocean, c is around 2.8 m/s. In our study where the East Indian Ocean influence is major, such a wave would take around 10 days to travel from this region to the coast of Sumatra. The first Indian influence on Lombok velocity is seen 15 days after a wind burst, this lag is coherent with Kelvin waves being responsible for propagation of wind energy toward the straits.

Conclusion

Intraseasonal variability in Lombok and Ombai passages seem to be driven in a large part by both local and remote wind forcings. The upper layer (0-80m) responds to wind stress over Flores and Sumba Seas presumably via an Ekman effect. Next layer (100-300m in Lombok, 100-700m in Ombai) is more influenced by the wind stress over eastern part of the equatorial Indian Ocean. Kelvin waves are probably responsible for the propagation of temperature and velocity anomalies to the strait along the equator and along the coasts of Sumatra, Java and Flores islands. Along this pathway waves would encounter a 300m-deep sill to reach Lombok moorings and a 800m-deep one to reach Ombai passage. Maximum correlations between wind stress or SLA and variables of the flow fade and change lag around these depths showing the importance of these straits in the propagation of Kelvin waves.

In Timor records it is harder to figure out the importance of wind forcings in the variability. Only the deep part of the sill shows a response to East Indian wind stress.

Wind stress over the Pacific Ocean doesn't appear on ISV in the region. However we only kept lagged correlation with a maximum lag of 60 days but Pacific Ocean could show influences on longer lags.

6. Conclusion, Perspectives for later researches

☉ Main results:

The present study's intent was to understand Intraseasonal Variability of the Indonesian Throughflow and to illustrate its relationships with the wind stress and altimetry fields. Important results are remembered here.

We confirmed the geographic differences of behaviour between Timor and Lombok/Ombai variability in temperature and velocity.

Lombok and Ombai straits undergo a major influence of East Indian Ocean for the deep variability while a surface layer is more influenced by local winds.

Intraseasonal Variability is partly formed by strong isolated events that can be forced by local Ekman effect or remote Kelvin wave excited by wind bursts over equatorial oceans.

Shallow flows in Timor passage do not correlate well with any wind stresses; eddies may play a larger role in this strait.

☉ Further studies:

These results will mainly be used to give a first idea of the characteristics of the variability while working on the whole length records. The three year records will be available at the beginning of 2007, analysis performed on a longer set of data will improve the statistical reliability of these results.

To better understand the physics it would be of great interest to use model outputs that give the velocity at all depths and everywhere: we could this way picture the deep penetrating behaviour of the waves and gain more understanding in the phenomena of Kelvin wave dispersion.

Another source of data to use is XBT profiles that already exist in the region and would give details on the structure of the variability in open water.

☉ Personal interest:

First of all I learnt the importance of pre-processing data before any analysis or interpretation could be performed on it.

I gained experience in processing temporal and spatial data from sensors and correlating variables. Most operations requiring programming were performed using Matlab, I thus learnt to master this programming language.

Finally I learnt some aspects of working in a research team and the importance of personal initiative in research.

Acknowledgments:

I am grateful to Dr Susan Wijffels who supervised my work in CSIRO Marine and Atmospheric Research in Hobart for all her attention and advices. I also thank Pr Robert Molcard who oriented me before this internship.

References:

Publications:

- [1]** - Potemra J., Hautala S., Sprintall J., and Pandoe W., 2002: *Interaction between the Indonesian Seas and the Indian Ocean in observations and numerical models*. Journal of Physical Oceanography, 32, 1838-1854.
- [2]** - Sprintall, Wijffels, Gordon, Molcard, 2004: *INSTANT: A new international array to measure the Indonesian Throughflow*. American Geophysical Union, Vol. 85, No. 39, p369-376.
- [3]** - Wijffels S. and Meyers G., 2003: *An intersection of Oceanic Waveguides: Variability in the Indonesian Throughflow Region*. Journal of Physical Oceanography, Vol. 34, 1232-1253.
- [4]** - Thompson Rory, 1983: *Low-Pass Filters to Suppress Inertial and Tidal Frequencies*, Journal of Physical Oceanography, Vol. 13, 1077-1083.

Books:

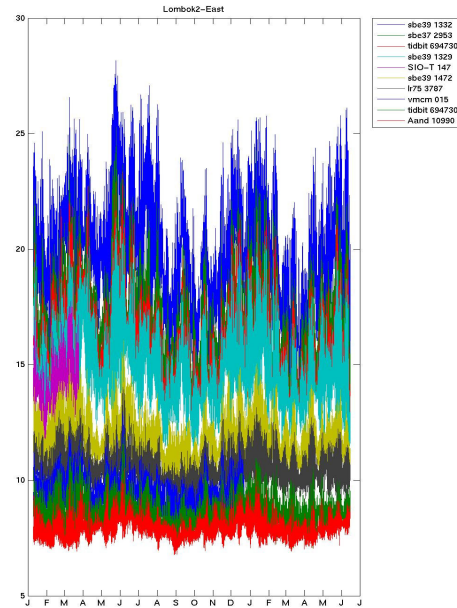
- [5]** - William J. Emery, Richard E. Thomson: *Data analysis methods in physical oceanography*; ed Pergamon. 371-551.
- [6]** - Gill A. E.; *Atmosphere-Ocean Dynamics*; International Geophysics Series. 371-482.
- [7]** - Kessler W. S., 2005: *Intraseasonal Variability in the Atmosphere-Ocean Climate System*, W.K.M. Lau and D.E. Waliser, Eds., Springer-Verlag, Berlin, 175-222.
- [0]** - Matlab help !

Annex

Some figures that can be useful to understand better the operation performed on the data or to visualize some simple results mentioned in the text.

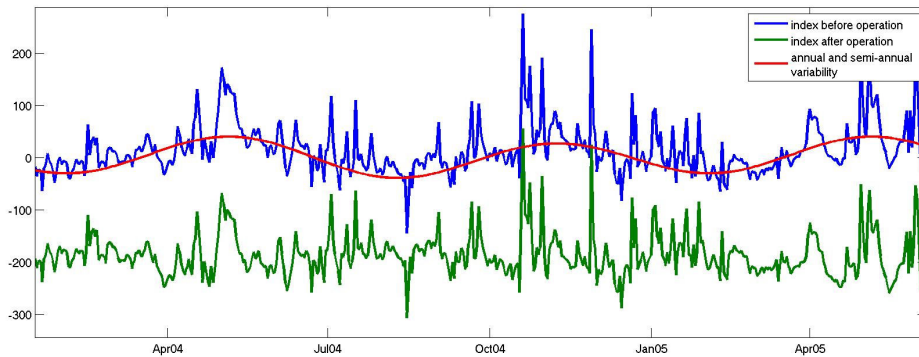
-1-

This figure shows the raw temperature data measured by the different sensors versus time in Lombok East. We remark the strong oscillations of depth (and thus temperature) mainly on the tidal frequencies. Some records stop early and it is preferable not to include the data at these depths in the analysis since it triggers further problems of trends and frequency analysis.



-2-

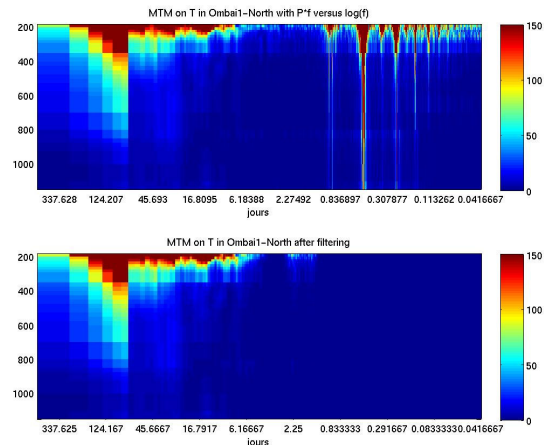
Example of the effect of subtracting annual and semi-annual cycles from a zonal wind stress index ($\cdot 10^{-2}$ Pa) over central Indian Ocean



-3-

These figures illustrate the effect of filtering the high frequencies in the spectral domain. We can point out that the operation really suppressed all energy in the high frequencies and didn't modify the amount of variance in low frequency bands.

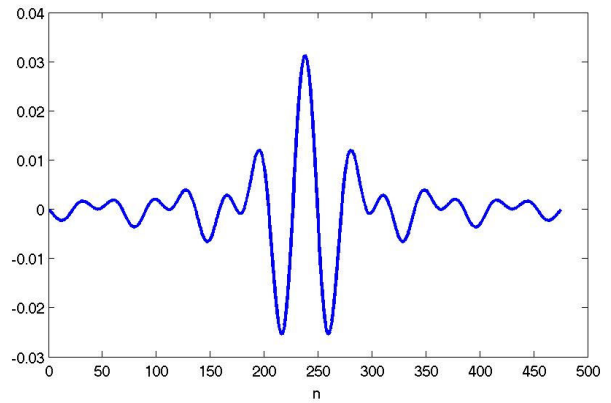
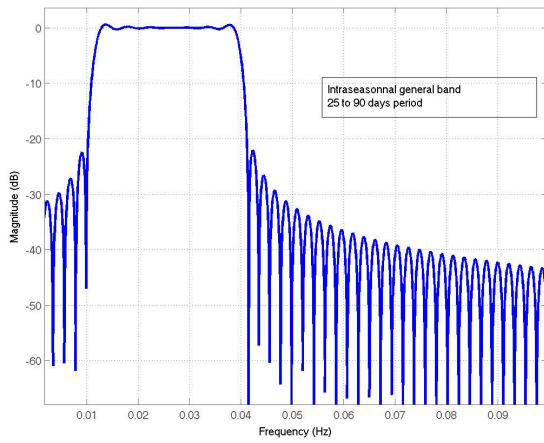
Annex 3 – Power spectra with depth before and after applying high frequency killing filter (Ombai N)



-4-

Annex 4a – Frequency response of the filter of the 25 to 90 days period band.

Annex 4b – Set of weights (Impulse Function) of the 35 to 65 days period band filter; here the length of the filter is 475.



-5-

This figure represents the coherence and associated phase shifts of temperature in Ombai North taking as a reference the 250m deep layer. It illustrates the different behaviour of the coherence between low (coherent on a huge depth) and high frequencies (lose coherence quickly).

